

EPJ Web of Conferences **40**, 18002 (2013)
DOI: 10.1051/epjconf/20134018002
© Owned by the authors, published by EDP Sciences, 2013

Anisotropic spin-orbit induced splitting of intersubband spin plasmons

F. Baboux^{1,a}, F. Perez¹, C. A. Ullrich², I. D'Amico³, J. Gómez¹, and M. Bernard¹

¹ Institut des Nanosciences de Paris, CNRS/Université Paris VI, Paris 75005, France

² Department of Physics and Astronomy, University of Missouri, Columbia, Missouri 65211, USA

³ Department of Physics, University of York, York YO10 5DD, United Kingdom

Abstract. The anisotropic splitting of intersubband spin plasmons, resulting from spin-orbit coupling, is studied by angle-resolved inelastic light scattering on a [001]-oriented GaAs/AlGaAs quantum well. Confirming theoretical predictions made in [C. A. Ullrich and M. A. Flatté, Phys. Rev. B **68**, 235310 (2003)], this splitting is proven to exhibit a characteristic two-fold symmetry with the in-plane orientation, and to increase with increasing modulus of the excitation momentum. This opens the way to a more complete investigation, aiming at evidencing the existence of a collective spin-orbit field driving these excitations.

1 Introduction

Spin-orbit (SO) coupling arises from special relativity: in the reference frame of a moving electron, electric fields transform into magnetic fields, acting on the spin. In zincblende type crystals such as GaAs, intrinsic electric fields arise from the lack of inversion center of the bulk material [1]. In a heterostructure such as a quantum well, additional intrinsic electric fields result from the structural inversion asymmetry [2]. The respective Dresselhaus and Rashba SO fields imprint the underlying heterostructure anisotropy onto the single- and many-particle properties of the carriers [3].

At the single-particle level, the main effect of SO coupling is a \mathbf{k} -dependent spin splitting and spin orientation of the conduction electron states. Following early experimental evidence of this splitting [4, 5], recent experiments were able to separately measure Rashba and Dresselhaus fields in the same sample [6–8], and the related anisotropy of the g -factor and of the spin relaxation. Also, these \mathbf{k} -dependent SO fields were demonstrated to be the major source of spin dissipation in doped quantum wells: If a spin coherence is created, e.g. by aligning the individual spins of the electron gas, each spin will then precess with a proper direction and rate, and the memory of the initial state will progressively be lost by decoherence. This single-particle effect is referred to as D'yakonov-Perel' dephasing [9].

By contrast, studies of SO effects at the many-body level are much more preliminary, although they are expected to reveal a rich spectrum of phenomena [10]. So far, the interplay between SO and Coulomb interactions was proven to produce consequent enhancements of the SO coupling constants [11] and of the g -factor [12]. On the other hand, Coulomb interaction was shown to reduce D'yakonov-Perel' dissipation via the additional momentum scattering [13, 14] and the exchange field [13, 15] it produces.

In line with the latter studies, we here aim at bringing insight into the *collective spin dynamics of interacting*

electrons in SO fields. To evidence such effects, we focus on a type of collective spin excitation which is formed by a coherent superposition of electronic transitions between the confinement-induced conduction subbands of a quantum well. The very existence of such intersubband spin-density excitations – hereafter denoted ISB spin plasmons – relies on exchange-correlations effects (beyond the standard Random Phase Approximation), that shift the excitation's energy away from that of single-particle excitations [16–18]. This makes these excitations ideally suited to study the interplay of Coulomb and spin-orbit interactions.

In Refs [19, 20], it was theoretically shown that by contrast with *intrasubband* spin-density excitations, such excitations were immune against D'yakonov-Perel' dissipation. Indeed, although they involve electrons with various momenta \mathbf{k} , thus experiencing, in a single-particle picture, non-equal SO fields, many-body effects make the \mathbf{k} -average of these fields vanish for an occupation number symmetric in \mathbf{k} , due to time-reversal symmetry. In the long-wavelength limit, an ISB spin plasmon would thus consist of a collective precession or oscillation of the magnetization, with no SO-induced dissipation. Apart from pointing out a good candidate for spin-based information transport, this situation would offer a privileged way to study the impact of electronic interactions on the dissipation. Indeed, for high-mobility 2D electron gases at low temperature, the dominant source of dissipation would be the spin Coulomb drag [21–23], an unavoidable friction between both spin populations.

2 Calculation of the spin plasmons dispersion in presence of spin-orbit coupling

The general structure of the ISB plasmon dispersions consists, without taking SO interaction into account, of a charge plasmon branch above, and a spin plasmon branch below the region of single-particle excitations. SO coupling is expected [19, 20] to split the spin plasmon branch into three

^a e-mail: baboux@insp.upmc.fr

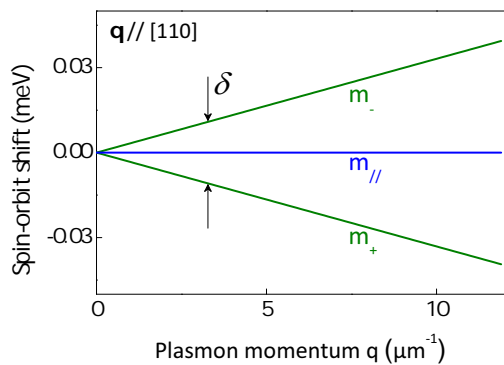


Fig. 1. Calculated dispersion of the intersubband spin plasmon modes. It is plotted as the difference of the mode energies with and without SO coupling (“spin-orbit shift”), with the parameters of the studied GaAs quantum well as an input. The splitting δ between the transverse m_{\pm} modes is almost linear with the magnitude q of the plasmon momentum (here $\mathbf{q} \parallel [110]$).

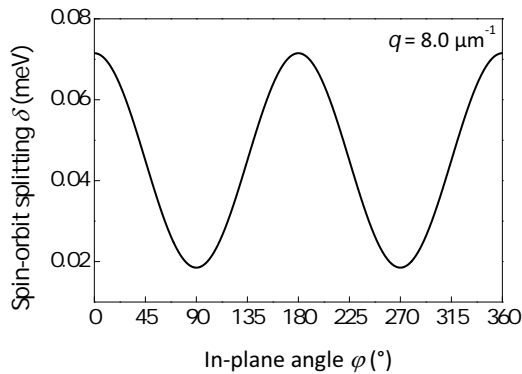


Fig. 2. Calculated modulation of the spin-orbit splitting δ as a function of the in-plane orientation of \mathbf{q} (labelled by the angle φ to $[110]$), for a fixed momentum modulus $q = 8.0 \mu\text{m}^{-1}$.

modes: one longitudinal oscillation mode, denoted m_{\parallel} , and two transverse precession modes, m_{+} and m_{-} [see Fig. 1]. The oscillating mode (m_{\parallel}) is a spin-conserving mode, whose energy is quasi-unaltered by SO effects. By contrast, the precession modes (m_{+}, m_{-}) are spin-flip modes, that are shifted in opposite directions by SO effects. Thus, a splitting δ appears between both transverse modes. This splitting varies with the excitation momentum \mathbf{q} , as a specific signature of the interference of Dresselhaus and Rashba effects in the quantum well.

In this communication, we aim at experimentally verifying two of the predictions made in Refs. [19, 20]:

- For a given orientation of \mathbf{q} , the SO splitting increases with increasing modulus of \mathbf{q} , as seen in Fig. 1 calculated for the GaAs quantum well that we will experimentally study;
- For a fixed modulus of \mathbf{q} , the splitting is modulated with the in-plane orientation of \mathbf{q} (labelled by the angle φ to $[110]$), exhibiting a characteristic two-fold symmetry, as seen in Fig. 2.

3 Experimental results

3.1 Sample and experimental setup

The studied sample is an asymmetrically modulation-doped GaAs/Al_{0.3}Ga_{0.7}As quantum well, grown along the $[001]$ direction by molecular beam epitaxy. The 200 Å-thick well was doped with two Si delta layers, separated from the well by spacer thicknesses of 350 and 400 Å respectively. The electron density is $2.3 \times 10^{11} \text{ cm}^{-2}$, and the mobility $2 \times 10^7 \text{ cm}^2 \text{ V}^{-1} \text{ s}^{-1}$ at the working temperature $T \approx 2 \text{ K}$ (superfluid Helium), as determined from Hall measurements.

We use resonant inelastic light scattering (ILS) [16, 24]. The experimental setup is in the backscattering geometry depicted in Fig. 3. The average angle θ of the incoming and backscattered light with respect to the normal direction can be changed to transfer a momentum \mathbf{q} of amplitude ranging from 0 to about $16 \mu\text{m}^{-1}$ ($\sim 15\%$ of the Fermi momentum). The in-plane angle φ between \mathbf{q} and the direction $[110]$ can be varied by rotating the sample holder about the growth axis of the sample.

Measurements are performed in a pumped-Helium optical cryostat. The sample is probed with a Coherent monolithic block resonator (MBR) single-mode Ti:Sapphire tunable ring laser with a wavenumber stability of better than 0.01 cm^{-1} . The scattered light is dispersed by a Dilor XY triple Raman spectrometer in additive mode and recorded with a nitrogen-cooled CCD multichannel detector. The experimental resolution is close to 0.02 meV . The exciting wavelength ($\lambda \approx 770 \text{ nm}$) is tuned in resonance with the lowest excitonic transition of the quantum well.

3.2 Evidence of the anisotropic spin-orbit induced splitting

Figure 4 shows typical intersubband ILS spectra obtained for $q = 8.0 \mu\text{m}^{-1}$ and $\varphi = 0^\circ$, in two different scattering configurations. The so-called polarized spectrum (orange) is obtained when the incident and scattered photons have parallel linear polarizations, while the depolarized spectrum (blue) is obtained when they have orthogonal linear polarizations. Owing to selection rules [16], the charge plasmon is seen in the polarized geometry, while the spin plasmon shows up in the depolarized geometry. The single-particle excitations continuum appears in both geometries (here as a small bump centered at about 30 meV). Note that the small peak near 30.5 meV in the depolarized spectrum arises from a small polarization leakage of our setup, that creates a slight departure from selection rules.

Now we focus on the spin plasmon peak, seen in the depolarized geometry where only the transverse modes, m_{+} and m_{-} , are active. Since q is non-zero, one would expect to see two slightly separated peaks, according to Fig. 1. However, a single, quasi-Lorentzian peak is observed, of full width at half maximum (FWHM) w . But by recording a series of spectra for various in-plane angles φ and by plotting w versus φ [Fig. 5(b)], w is modulated quasi-sinusoidally with a period π . This modulation is characteristic of the two-fold symmetry as the SO splitting δ (Fig. 2), with a maximum along $[110]$ ($\varphi = 0^\circ$) and a minimum along $[\bar{1}10]$ ($\varphi = 90^\circ$).

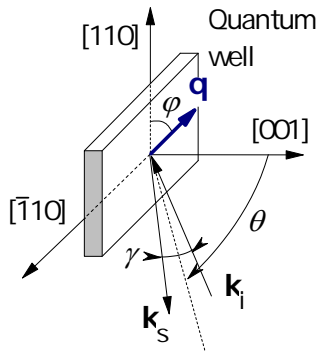


Fig. 3. Geometry of our angle-resolved inelastic light scattering setup, showing angle definitions (see text). \mathbf{k}_i and \mathbf{k}_s are the incoming and scattered light wavevectors. The transferred momentum \mathbf{q} reads $q = \frac{4\pi}{\lambda} \cos \frac{\gamma}{2} \sin \theta$, with $\lambda \approx 770$ nm the exciting wavelength.

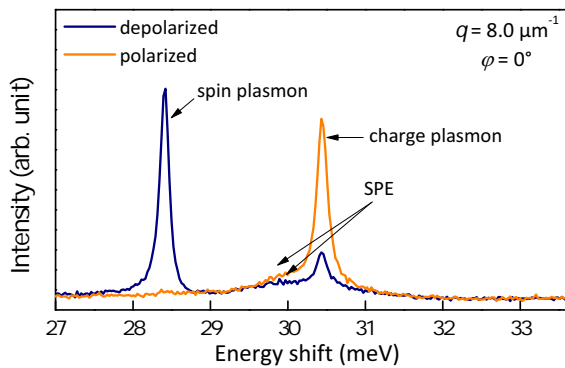


Fig. 4. Inelastic light scattering spectrum of the intersubband excitations for $q = 8.0 \mu\text{m}^{-1}$ and $\varphi = 0^\circ$, obtained in polarized (orange) and depolarized (blue) geometry. The spin plasmon peak appears in the depolarized geometry only, and is well separated from the single-particle excitations (SPE) continuum, that appears in both configurations.

Furthermore, by repeating the same experiments for $q = 5.4 \mu\text{m}^{-1}$ and $q = 10.2 \mu\text{m}^{-1}$ [Fig. 5(a)-(c)], we find that the amplitude of the modulation decreases with decreasing q , in qualitative agreement with Fig. 1(a).

Both observations, taken together, confirm the spin-orbit origin of the modulation. The reason why we do not resolve two peaks is that the spin-orbit splitting δ is small in comparison with the FWHM of each peak, which is dominated by the spin Coulomb drag [21–23]. Thus, the m_+ and m_- peaks add up to form a composite peak. But since the FWHM is identical for both modes and quasi-independent on φ [21,22], the variation of the linewidth w of this composite peak with φ reflects that of the splitting δ , where the amplitude of the modulation increases with the wavevector. A fully quantitative comparison with the theoretical data of Fig. 2 is provided in Ref. [25].

4 Future work

Our results strongly suggest that, as predicted by Refs. [19, 20], the effect of SO coupling on ISB spin plasmons shows

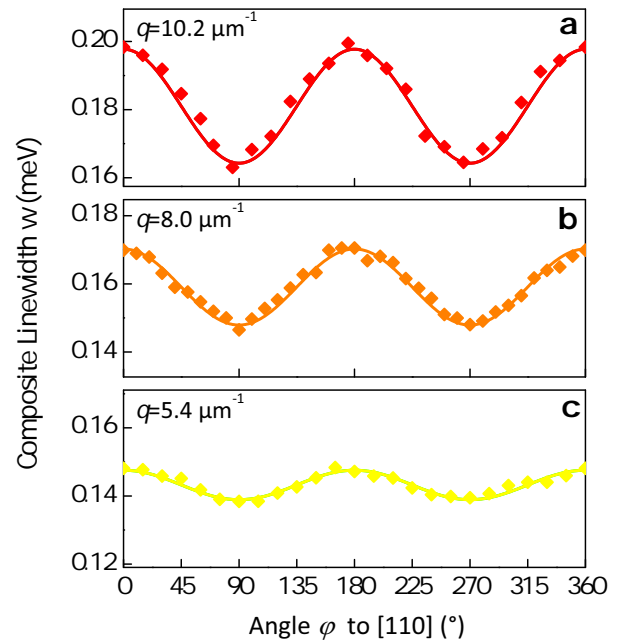


Fig. 5. Variation of the composite linewidth w (FWHM) of the spin plasmon peak with the in-plane orientation of \mathbf{q} (measured from [110]), obtained for $q = 10.2, 8.0$ and $5.4 \mu\text{m}^{-1}$. The 180-degree period, as well as the increasing amplitude of the modulation with q , are in qualitative agreement with the calculations of Figs. 1 and 2.

up as a clear-cut splitting of the transverse modes, modulated with the in-plane angle, and increasing with the amplitude of the excitation momentum.

Both characteristics point to the possible existence of a collective spin-orbit effective field associated with the spin plasmons. One can think of it in the following way. The probed ISB spin plasmons involve transitions between spin states with momentum \mathbf{k} from the fundamental subband ($n = 1$), and states with momentum $\mathbf{k} + \mathbf{q}$ from the first excited subband ($n = 2$) of the quantum well. Let $\mathbf{B}_{\text{SO},n}(\mathbf{k})$ denote the magnetic field seen by an electron of momentum \mathbf{k} in the n -th subband. During their transition, electrons experience the magnetic field difference $\mathbf{B}_{\text{SO},2}(\mathbf{k} + \mathbf{q}) - \mathbf{B}_{\text{SO},1}(\mathbf{k})$. This one-particle field depends on \mathbf{k} , so that one could expect a D'yakonov-Perel' decoherence mechanism acting on the spin plasmons.

However, the D'yakonov-Perel' picture is valid only for single-particle dynamics, while we here deal with a collective excitation whose coherence is created by Coulomb interactions between electrons. And indeed, in the frame of time-dependent density functional theory, coulombic effects were shown to exactly compensate the \mathbf{k} -dependence of $\mathbf{B}_{\text{SO},2}(\mathbf{k} + \mathbf{q}) - \mathbf{B}_{\text{SO},1}(\mathbf{k})$. These many-body effects could give rise to a collective uniform SO field $\mathbf{B}_{\text{SO}}^{\text{coll}}(\mathbf{q})$, about which the spins of the interacting electrons would either oscillate (longitudinal mode) or precess (transverse modes). Although challengingly difficult to calculate, this field might be probed with our ILS scheme, by using external magnetic fields.

Acknowledgements

F.B and F.P. thank M. Bernard and S. Majrab for technical support and B. Jusserand for fruitful discussion. F.P. acknowledges funding from C’NANO IDF 2009 (SPIN-WAVEDYN) and ANR 2007 (GOSPININFO). F.B. is supported by a Fondation CFM-JP Aguilar grant. I.D’A. acknowledges support from EPSRC Grant No. EP/F016719/1 and I.D’A. and F.P. acknowledge support from Royal Society Grant No. IJP 2008/R1 JP0870232. C.A.U. is supported by DOE Grant No. DE-FG02-05ER46213.

References

1. G. Dresselhaus, Phys. Rev. **100**, 580 (1955).
2. Y. Bychkov and E. I. Rashba, J. Phys. C **17**, 6039 (1984).
3. R. Winkler, *Spin-Orbit Coupling Effects in Two-Dimensional Electron and Hole Systems* (Springer, Berlin, 2003).
4. B. Das, D. C. Miller, S. Datta, R. Reifenberger, W. P. Hong, P. K. Bhattacharya, J. Singh, and M. Jaffe, Phys. Rev. B **39**, 1411 (1989).
5. P. D. Dresselhaus, C. M. A. Papavassiliou, R. G. Wheeler, and R. N. Sacks, Phys. Rev. Lett. **68**, 106 (1992).
6. L. Meier, G. Salis, I. Shorubalko, E. Gini, S. Schon, and K. Ensslin, Nature Phys **3**, 650 (2007).
7. M. Studer, G. Salis, K. Ensslin, D. C. Driscoll, and A. C. Gossard, Phys. Rev. Lett. **103**, 027201 (2009).
8. P. S. Eldridge, J. Hübner, S. Oertel, R. T. Harley, M. Henini, and M. Oestreich, Phys. Rev. B **83**, 041301(R) (2011).
9. M. D’yakonov and V. Perel’, Sov. Phys. Solid State **13** (1971).
10. A. Agarwal, S. Chesi, T. Jungwirth, J. Sinova, G. Vignale, and M. Polini, Phys. Rev. B **83**, 115135 (2011).
11. G.Q. Liu, V. N. Antonov, O. Jepsen, and O. K. Andersen, Phys. Rev. Lett. **101**, 026408 (2008).
12. B. Nedniyom, R. J. Nicholas, M. T. Emeny, L. Buckle, A. M. Gilbertson, P. D. Buckle, and T. Ashley, Phys. Rev. B **80**, 125328 (2009).
13. M. Glazov and E. Ivchenko, Journal of Experimental and Theoretical Physics **99**, 1279 (2004).
14. W. J. H. Leyland, G. H. John, R. T. Harley, M. M. Glazov, E. L. Ivchenko, D. A. Ritchie, I. Farrer, A. J. Shields, and M. Henini, Phys. Rev. B **75**, 165309 (2007).
15. D. Stich, J. Zhou, T. Korn, R. Schulz, D. Schuh, W. Wegscheider, M. W. Wu, and C. Schüller, Phys. Rev. B **76**, 205301 (2007).
16. A. Pinczuk, S. Schmitt-Rink, G. Danan, J. P. Val-ladares, L. N. Pfeiffer, and K. W. West, Phys. Rev. Lett. **63**, 1633 (1989).
17. D. Gammon, B. V. Shanabrook, J. C. Ryan, and D. S. Katzer, Phys. Rev. B **41**, 12311(R) (1990).
18. J. M. Bao, L. N. Pfeiffer, K. W. West, and R. Merlin, Phys. Rev. Lett. **92**, 236601 (2004).
19. C. A. Ullrich and M. E. Flatté, Phys. Rev. B **66**, 205305 (2002).
20. C. A. Ullrich and M. E. Flatté, Phys. Rev. B **68**, 235310 (2003).
21. I. D’Amico and G. Vignale, Phys. Rev. B **62**, 4853 (2000).
22. I. D’Amico and C. A. Ullrich, Phys. Rev. B **74**, 121303(R) (2006).
23. C. P. Weber, N. Gedik, J. E. Moore, J. Orenstein, J. Stephens, and D. D. Awschalom, Nature **437**, 1330 (2005).
24. F. Perez, C. Aku-leh, D. Richards, B. Jusserand, L. C. Smith, D. Wolverson, and G. Karczewski, Phys. Rev. Lett. **99**, 026403 (2007).
25. F. Baboux, F. Perez, C.A. Ullrich, I. D’Amico, J. Gómez, and M. Bernard, Phys. Rev. Lett. **109**, 166401 (2012).